

Traffic Measurement and Vehicle Classification with a Single Magnetic Sensor

*Sing Yiu Cheung, Sinem Coleri, Baris Dundar, Sumitra Ganesh, Chin-Woo Tan and Pravin Varaiya**

University of California, Berkeley, CA 94720-1770
Tel: (510) 642-5270, Fax: (510) 642-7615
singyiu@path.berkeley.edu, {csinem,dundar,sumitra,tan,varaiya}@eecs.berkeley.edu

For Presentation and Publication
84th Annual Meeting
Transportation Research Board
January 2005
Washington, D.C.

July 18, 2004

Words: 4,110 (excluding Figure and Table captions)
Plus 1 Table and 11 Figures (2,900)
TOTAL: 7,010

*Corresponding Author

ABSTRACT

Wireless magnetic sensor networks offer a very attractive, low-cost alternative to inductive loops for traffic measurement in freeways and at intersections. In addition to vehicle count, occupancy and speed, these sensors yield information (such as non-axle-based vehicle classification) that cannot be obtained from standard loop data. Because such networks can be deployed in a very short time, they can also be used (and reused) for temporary traffic measurement.

This paper reports the detection capabilities of magnetic sensors, based on two field experiments. The first experiment collected a two-hour trace of measurements on Hearst Avenue in Berkeley. The vehicle detection rate is better than 99 percent (100 percent for vehicles other than motorcycles); and estimates of average vehicle length and speed appear to be better than 90 percent. The measurements also yield inter-vehicle spacing or headways, which reveal such interesting phenomena as platoon formation downstream of a traffic signal.

Results of the second experiment are preliminary. Sensor data from 37 passing vehicles at the same site are processed and classified into six types. Sixty percent of the vehicles are classified correctly, when length is *not* used as a feature. The classification algorithm can be implemented in real time by the sensor node itself, in contrast to other methods based on high scan-rate inductive loop signals, which require extensive offline computation. We believe that when length is used as a feature, 80-90 percent of vehicles will be correctly classified.

Keywords: wireless sensors, traffic measurement, vehicle classification, advanced traffic management systems

1. INTRODUCTION

Wireless magnetic sensor networks offer a very attractive alternative to inductive loops for traffic measurement in freeways and at intersections in terms of cost, ease of deployment and maintenance, and enhanced measurement capabilities. These networks consist of a set of sensor nodes (SN) and one access point (AP). A SN comprises a magnetic sensor, a microprocessor, a radio, and a battery. Each SN is encased in a 5"-diameter 'smart stud' that is glued to the center of a lane.

A SN is self-calibrating. Sensor measurements are processed within the SN and the results are transmitted via radio to the AP, located on the roadside. The AP, housed in a 3"x5"x1" box attached to a pole or the controller, comprises a radio, and a more powerful processor. It processes the data received from the SNs. The results are sent to a local controller or to the TMC. The AP is either line- or solar-powered. Figure 1 shows how such a network might be deployed. The little circles are the SNs, the square is the AP.

Wireless sensing has the potential to revolutionize the way information is collected for various transportation applications by providing measurements with high spatial density and accuracy. A network of wireless magnetic sensors offers much greater flexibility and lower installation and maintenance costs than loop, video and radar detector systems. The suitability for large-scale deployment of such networks makes it possible to collect traffic data that are presently not available, but are needed to analyze and control a transportation system. The availability of these data generates a new window of research opportunities for signal processing, communications, traffic operations and control.

The paper focuses on the extraction of information from experimentally obtained magnetic measurements. A sensor network implements two functions: detection and measurement, and communication. Communication is discussed in [1]. The paper discusses the experiments and how well a magnetic sensor can detect vehicles and estimate various traffic parameters.

Two experiments were performed. The first provides a two-hour trace of measurements on Hearst Avenue, Berkeley, CA, downstream of a signalized intersection. In all 332 vehicles were observed. The results are excellent: detection rate of 99% (100% if motorcycles are excluded), and average vehicle length and speed estimates that appear better than 90%. Because the sensor detects individual vehicles rather than 30-sec averages, analysis yields additional information, such as inter-vehicle headways and the formation of platoons downstream of a signal.

The second experiment is more limited and the results are less definitive. Magnetic 'signatures' from 37 vehicles are processed to classify them into six types. The algorithm achieves a 60 percent correct classification rate in *real time*, *without* using vehicle length. The correct classification rate should increase to 80-90 percent after incorporating length. Sections 2 and 3 present the results of the experiments. Section 4 compares magnetic signatures with high scan-rate inductive loop signatures. Section 5 discusses the results and outlines future work. Section 6 concludes the paper.

2. VEHICLE DETECTION

One sensor node was placed in the middle of one lane of Hearst Avenue, Berkeley, CA, on February 23, 2004, 8-9 pm. Ground truth was established by a visual count. In all 332 vehicles were observed: Passenger vehicles (248); SUVs (48); Vans (18); Mini-trucks (9); Buses (4); and Motorcycles (5).

Detection rate

The node detected 330 (99%) vehicles. The two undetected vehicles were motorcycles, so all non-motorcycle vehicles are detected. A motorcycle that passes near the node *is* detected, so placing two nodes will ensure motorcycle detection.

The sensor measures $mag(z)$, the magnetic field in the vertical direction, sampled at 128Hz, or 128 times per second. The samples are compared with a threshold, resulting in a sequence of 1's and 0's. If 10 successive values are 1 (above the threshold), vehicle detection is declared. When the sample values subsequently fall below the threshold for 0.25s, the vehicle is declared to have passed the sensor. The state machine coded in the SN processor sets a detection flag whose value is 1 for the time during which a vehicle is above the sensor, and whose value is 0 otherwise. Figure 2 displays the raw samples (left) from the passage of a single vehicle and the corresponding detection flag (right).

Vehicle arrivals

As successive vehicles pass over the sensor, the detection flag produces a corresponding sequence of pulses. When the flag switches from 0 to 1 is its *uptime*, and when it switches from 1 to 0 its *downtime*. The interval between an uptime and the subsequent downtime is the *ontime*.

At a finer scale Figure 2 would show that the uptime occurs within 10 samples, i.e. in less than 0.1s immediately after the front of the vehicle just crosses the sensor. Thus the presence of a vehicle can be reported within 0.1s to the controller. The sum of the ontimes over a 30s interval divided by 30 is the occupancy of a loop detector.

Thus a single sensor node produces measurements obtained from a single inductive loop in signal control and freeway traffic monitoring applications. Moreover, these measurements are made without a detector card used by a loop detector.

In fact, more information can be extracted because each vehicle is *individually* measured. Each uptime indicates the arrival of a vehicle at the sensor. Figure 3 is a plot of vehicle arrivals during the first 10 minutes. (The entire two hour-long trace is not plotted, because the scale would be too small.) Each cross is the time when a vehicle crosses the node. The arrivals are bunched together in 'platoons' formed by the clearing of the queue behind the signal during each green phase. Successive platoons are one minute apart, which is the cycle time. The variability in platoon size implies that traffic is not saturated—the queue is cleared during each green phase. Typical signal control detection systems do not measure traffic downstream of a signal. But the figure shows that such measurements can reveal how well the signal plan is adapted to the traffic demand. The information in the figure is produced in real time by the sensor node itself, with no additional processing.

The sensor nodes can be deployed in an arbitrary configuration to collect information for adaptive signal control [13]; for example, queue lengths at intersections can be measured by placing SNs as far upstream of the signal as needed.

Average vehicle length and speed

The *ontime* or interval between successive uptime and downtime of the detection flag is the time during which a vehicle is above the sensor. Consider n successive vehicles, with measured ontimes t_1, t_2, \dots, t_n . (To fix ideas, take $n = 11$, for reasons argued by Coifman et al. [3].) Suppose the unknown lengths of these vehicles (in meters) are l_1, l_2, \dots, l_n , and their (assumed) common but unknown speed is v (m/s). The $n+1$ unknowns l_1, l_2, \dots, l_n and v satisfy n equations,

$$(1) \quad l_i = t_i \times v, \quad i = 1, \dots, n.$$

If the distribution $p(l)$ of vehicle lengths is known, one can obtain a maximum likelihood estimate of the vehicle speed \hat{v} , and the vehicle lengths

$$(2) \quad \hat{l}_i = t_i \times \hat{v}, \quad i = 1, \dots, n.$$

As shown in [3], a robust estimate of the speed v is easily calculated as

$$(3) \quad \bar{v} = \frac{\bar{l}}{\bar{t}},$$

wherein \bar{l} is the *median* vehicle length and \bar{t} is the *median* of the n observed ontimes t_1, t_2, \dots, t_n . We adopt this procedure, choosing $n = 11$ (as suggested in [3]) and also $n = 5$, for purposes of comparison. We take the median vehicle length as $\bar{l} = 5$ meters.

Figure 4 displays the 5-point and 11-point median vehicle speed estimates. The 11-point estimate is smoother as expected. With traffic flowing at 330 v/hr, the passage of 11 vehicles takes about 2 minutes, so the 11-point estimate corresponds to a 2-min average. Under a heavier traffic flow, say 2,000 v/hr, this would be a 20-second average.

The headway is obtained if we subtract from the uptime (arrival) of a vehicle the downtime (departure) of the preceding vehicle. Figure 5 plots the headway in seconds for the first 10 minutes: The signal light creates departures in platoons, separated by large headways.

Using the speed estimate \bar{v} for \hat{v} in (2) the vehicle length estimates are

$$(4) \quad \hat{l}_i = t_i \times \bar{v}, \quad i = 1, \dots, n.$$

Figure 6 is the resulting frequency distribution of vehicle lengths.

Accuracy of estimates

For freeway data, Coifman et al. [3] find the standard deviation (σ) of a 10-point median speed estimate to be 2.5 mph. So with 0.95 probability the estimates differ from the true average speed by less than 2σ or 5 mph. We can measure the speed of an *individual* vehicle by placing two sensor nodes at a known distance. These measurements will be carried out in the future.

A better estimate of speed and length is provided by a maximum likelihood estimate, which requires knowledge of the length distribution $p(l)$. Alternatively, one can estimate this distribution, together with the speed.

3. VEHICLE CLASSIFICATION

One can estimate volumes of long vehicles (trucks) and short vehicles (cars) from 30-second average single-loop measurements of occupancy and counts [5][6]. However, classification of *individual* vehicles requires finer measurement.

This section reports results of a simple classification scheme based on a single dual-axis magnetic sensor, which measures the earth's magnetic field in both the vertical direction ($mag(z)$) and along the direction of the lane ($mag(x)$), each sampled at 64Hz or 64 times per second. A vehicle's samples (*signature*) are processed and two pieces of information are extracted. First, the rate of change of consecutive samples is compared with a threshold and declared to be +1 (-1) if it is positive and larger than (or negative with magnitude larger than) the threshold, or 0 if the magnitude of the rate is smaller than the threshold. The result is a 'hill pattern' of 'peaks' and 'valleys' in the vehicle's $mag(z)$ and $mag(x)$ signature. The second piece of information is the largest value of the samples. Although in the results reported below, the information was generated off-line, it can be extracted in real time by the sensor node itself. Information about vehicle length is *not* used.

A simple algorithm uses the information to classify the vehicle into six types: passenger vehicles (1), SUV (2), Van (3), Bus (4), mini-truck (5), truck (6), and other (7).

Figure 7 displays the signature and hill pattern from four passenger vehicles (PV). There are six plots per vehicle. The top row shows the signature, $mag(z)$ and $mag(x)$. The second row is the hill pattern. In each case the $mag(z)$ profile shows a single 'peak' constituting the hill pattern (+1,-1) or one positive slope followed by one negative slope. In each case the $mag(x)$ profile shows one 'valley' followed by one 'peak' constituting the hill pattern (-1,+1,-1). The third row gives the outcome of the algorithm, which classifies the signature into seven types. In each case the algorithm correctly decides that it is a passenger vehicle (type 1).

Figure 8 displays the signature, hill pattern and classification of four SUVs. In three cases (top two and bottom right) the patterns of both $mag(z)$ and $mag(x)$ are different from the passenger vehicle pattern of Figure 7. These patterns are (-1,+1,-1) and (+1, -1, +1, -1) respectively, both different from the type-1 pattern. However, the vehicle on the bottom left is misclassified as a passenger vehicle, because the initial negative slope of $mag(z)$ is too small in magnitude to cross the threshold, and $mag(x)$ does not show the initial positive slope of the three other signatures.

The misclassification may be due to several reasons. The two peaks in $mag(x)$ in the three correctly classified SUVs are due to two masses of steel (ferrous material) separated by a significant gap. Such a distribution of steel is not detected in the misclassified SUV. A higher sampling rate might reveal the 'missing' peak. It is also possible that this SUV is built differently from the others, making its signature similar to that of a passenger vehicle. Also, a lower $mag(z)$ threshold would reveal the small valley that is visible in

the raw samples. Lastly, if SUVs are longer than passenger vehicles, using length as a feature might lead to a correct classification.

Figure 9 displays the signature and hill pattern for four vans. Three vehicles are correctly classified as Type 6, and one is misclassified. The van hill pattern for $mag(z)$ is $(+1,-1,+1,-1)$ and for $mag(x)$ is $(-1,+1,-1)$ (the same as that of a passenger vehicle). The $mag(z)$ pattern for the misclassified vehicle does have the two peaks, but the first peak is too small to cross the threshold. Again, incorporation of length might have helped.

Similar hill patterns are obtained for the two remaining classes, buses and mini-trucks (MT).

Table 1 indicates that 24 out of 37 vehicles (63 percent) are correctly classified. The FHWA vehicle class 2 combines PV and SUV, class 3 combines Vans and MT, and class 3 comprises buses. From Table 1 we can see that 31 out of 37 vehicles (83 percent) are correctly identified in terms of the FHWA classes. Although the sample size is too small to make any firm judgment, the technique is very promising and suggests two tentative conclusions.

First, buses, vans and passenger vehicles are all correctly classified. The troublesome vehicles are SUVs and mini-trucks. The data do not contain any trucks, and further experiments will tell how well their signatures are distinguishable.

Second, the classification uses measurements from a *single* sensor, without using length as a feature, and the algorithm can be implemented in real time. All loop detector signature-based classification schemes reviewed in the next section require two loops (to extract speed and hence length) and require off-line computations.

4. COMPARISON WITH LOOP SIGNATURE-BASED CLASSIFICATION

We compare magnetic signature-based classification with three studies that use signatures from inductive loop signals scanned at a high rate (about 140 Hz). A survey of studies that use inductive loop signatures is provided in [2].

The studies use seven categories, slightly different from each other and from Table 1. The loop-based studies are all based on pattern recognition methods. All these studies use length as an important feature.

Two sets of schemes are tested in Sun [2]. The first, called ‘decision-theoretic’ methods, uses the features of length, largest magnitude of the measured inductance, variance and skewness (defined as the third or fourth central moment of the signal).

Significant pre-processing of the raw data is needed to extract the features. As explained in [2], [9]: (1) the signal magnitude must be normalized; (2) the ontime must be multiplied by speed to convert the time axis into length; and (3) a spline function must be interpolated through the raw samples and the result re-sampled so that each signature has an equal number of sample points.

The decision-theoretic methods use a heuristic ‘decision tree’ like the one shown in Figure 12. The procedure works as follows. The six thresholds b_1, \dots, b_6 are selected to give the best results for a ‘training set’ of vehicles. Length is compared with four

thresholds b_1, \dots, b_4 to give five regions, namely, $(0, b_1), (b_1, b_2), (b_2, b_3), (b_3, b_4), (b_4, \infty)$. If the length falls within the middle three intervals, the vehicle is immediately classified as Type 3, 4 or 5. If the length falls into the first interval, it is classified Type 1 or 2, and the magnitude of the signal is then compared with b_5 to resolve its type (1 or 2). Similarly, if the length is larger than b_4 , it is classified Type 6 or 7, and the ambiguity is resolved by comparing its skewness with the threshold b_6 . Evidently, length plays a dominant role in the classification.

The second set of classification schemes in [2] uses a neural network with additional features, including Discrete Fourier Transform and Karhunen-Loeve Transform coefficients. The final scheme uses a total of 51 features. Extracting these features requires much computation.

These schemes correctly classify 80 percent of the vehicles..

In summary, it appears that magnetic signatures are better than inductive-loop signatures in terms of (1) computational burden, (2) improved sensitivity (speed and length are not used), and (3) implementation. The improved sensitivity is explained next.

Magnetic sensor vs. inductive loop measurements

The sensor node uses the HMC 1001/1002 Honeywell chip, whose magneto-resistive sensors convert the magnetic field to a differential output voltage, capable of sensing magnetic fields as low as 30 μ gauss 0. (The earth's field is between 250 and 650 mGauss.) Ferromagnetic material, such as iron, with a large permeability, changes the earth's magnetic field. The voltage change is sampled at 128Hz to give the signature.

The magnetic field is a three-dimensional vector. The vehicle detection experiment uses only the field in the vertical direction, $mag(z)$; vehicle classification is based on both $mag(z)$ and $mag(x)$ —the change along the direction of the vehicle's motion. Figures 7–9 show some signatures.

The magnetic sensor is passive, and energy is consumed in the electronic circuit that measures the change in the resistance and the A/D conversion. By contrast, the inductive loop is an active device: a 6' by 6' copper loop is excited by a 20kHz voltage, creating a magnetic field. Conducting material passing over the loop lowers the inductance. The loop detector card measures the change in the inductance. Special high scan-rate detector cards used for vehicle classification sample the inductance at about 140Hz.

The tiny magnetic sensor measures a highly localized change. As the vehicle travels over the sensor, it records the changes in the fields caused by different parts of the vehicle. By contrast, the 6' by 6' standard loop geometry results in the "integration of the inductive signature over the traversal distance ... which can *remove distinctive features* from the inductive signature" [4, emphasis added]. So the standard loop is not ideal for vehicle classification. Figure 13 reproduces the inductive loop signatures of a pickup truck and a passenger car. Magnetic signatures clearly provide much more detail.

5. DISCUSSION AND FUTURE PLANS

The limited experiments reported here suggest that a magnetic sensor provides count accuracy exceeding 99 percent, and average vehicle speed and length estimates better than 90 percent. Moreover, a single (dual-axis) sensor can classify six types of vehicles with accuracy better than 60 percent. We believe that if two sensors are used, individual vehicle speeds can be very accurately measured, and vehicles can be classified with accuracy better than 80 percent. Significantly, all these estimates can be carried out in real time.

An earlier study [1] described a communication protocol that consumes so little power than a sensor node can be supplied by energy from two AA batteries for more than three years. More careful designs by Sensys Networks, Inc. indicate a lifetime exceeding seven years. (Full disclosure: Pravin Varaiya is a founder of Sensys.) The low-cost, ease of deployment and maintenance, and greater information of these sensor networks, suggest that they can serve as a foundation for an accurate, extensive, and dense traffic surveillance system.

For the immediate future, we plan to work in several directions. Experiments with two nodes six feet apart indicate speed estimates with an accuracy exceeding that obtained by a video camera (because the nodes provide a resolution of 128Hz vs. the 30Hz video frame rate). We will soon conduct extensive tests on freeways and arterials and compare the results with loop and video measurements. Accurate speed measurements yield accurate vehicle length. We will characterize the improvement in vehicle classification using length as a feature. We have obtained truck measurements at a weigh-in-motion station. We are developing a classification algorithm based on these data.

We believe that magnetic sensors can be placed on bridges and overpasses, where it is difficult to cut the pavement to install loop detectors. We plan to conduct such tests. The absence of detectors at these locations (where congestion often occurs) leaves a significant gap in freeway traffic monitoring.

Over the longer term, we will explore other sensing modalities, including temperature and fog sensors, and accelerometers. The interesting thing about the sensor network (figure 1) is that the same communication and node architecture can be used to process and communicate measurements from different sensors.

The PeMS project [12] has shown the value of traffic data for measuring and improving freeway performance. The project also shows how difficult it is to maintain California's loop detector system. Wireless sensor networks may provide the ideal low-cost, accurate traffic surveillance system needed to improve our transportation system.

6. CONCLUSIONS

Vehicle detection systems based on wireless sensor networks are attractive because of their low cost, ease of installation and flexibility of deployment. The paper examined their detection capability. The networks provide a detection rate of 99 percent; and achieve a 90 percent accuracy in average vehicle length and speed estimates with a single sensor. The localized change associated with the magnetic sensor allows us to classify the vehicles based on the magnetic signature without incorporating the length with 60 percent

accuracy. In the future, we plan to continue to work on the classification of the vehicles and different kinds of trucks, and perform extensive experiments on urban streets and freeways with multiple lanes and higher volumes.

ACKNOWLEDGEMENT

This work was supported by National Science Foundation Award CMS-0408627 and the California PATH Program of the University of California, in cooperation with the California Department of Transportation. The contents of this paper reflect the views of the authors who are responsible for the facts and the accuracy of the data presented herein. The contents do not necessarily reflect the official views or policies of the State of California.

REFERENCES

- [1] S. Coleri and P. Varaiya. PEDAMACS: Power efficient and delay aware medium access protocol for sensor networks. California PATH Working Paper UCB-ITS-PWP-2004-6, 2004.
- [2] C. Sun. An investigation in the use of inductive loop signatures for vehicle classification. California PATH Research Report UCB-ITS-PRR-2002-4, 2000.
- [3] B. Coifman, S. Dhoorjaty and Z.-H. Lee. Estimating median velocity instead of mean velocity at single loop detectors. *Transportation Research, Part C*, vol 11C, nos. 3-4, pp. 211-222, June-August 2003.
- [4] C. Oh, S.G. Ritchie and S.-T. Jeng. Vehicle re-identification using heterogeneous detection systems. 83rd TRB Annual Meeting, January 2004, Washington, D.C.
- [5] J. Kwon, A. Skabardonis and P. Varaiya. Estimation of truck traffic volume from single loop detector using lane-to-lane speed correlation. 82nd TRB Annual Meeting, January 2003, Washington, D.C.
- [6] X. Zhang, Y. Wang and N.L. Nihan. Monitoring a freeway network in real-time using single-loop detectors: System design and implementation. 83rd TRB Annual Meeting, January 2004, Washington, D.C.
- [7] S. Oh, S.G. Ritchie and C. Oh. Real time traffic measurement from single loop inductive signatures. 81st TRB Annual Meeting, January 2002, Washington, D.C.
- [8] A.N. Knaian. A wireless sensor network for smart roadbeds and intelligent transportation systems. M.S. thesis. Department of Electrical Engineering and Computer Science, MIT, Cambridge, MA, 2000.
- [9] B. Abdulbahai and S.M. Tabib. Spatio-temporal inductive-pattern recognition for vehicle re-identification. *Transportation Research, Part C*, vol 11C, nos. 3-4, pp. 223-240, June-August 2003.
- [10] J. Ding. Vehicle detection by sensor network nodes. MS thesis, Department of Electrical Engineering and Computer Science, University of California, Berkeley, CA, Fall 2003.

- [11] <http://www.honeywell.com/magnetic/datasheet/magsen.pdf>
- [12] <http://pems.eecs.berkeley.edu/>
- [13] L. Head. RHODES: Equipment requirements. TRB Traffic Signal Systems Committee: Workshop on Adaptive Signal Control Systems, January 2001, Washington, D.C.

List of Tables

TABLE 1 Classification using magnetic sensor

List of Figures

- Figure 1 Deploying sensor networks at intersection and freeway
- Figure 2 Raw samples and detection flag; time (x-axis) is in seconds
- Figure 3 Vehicle arrivals during the first 10 minutes
- Figure 4 Vehicle speed using 5-point and 11-point median
- Figure 5 Headway vs. arrival time
- Figure 6 Frequency distribution of vehicle length (m)
- Figure 7 Raw samples and hill pattern from four passenger vehicles
- Figure 8 Raw samples and hill pattern from four SUVs
- Figure 9 Raw samples and hill pattern from four vans
- Figure 10 Decision tree for classification into 7 types of vehicles: Source [2]
- Figure 11 Inductive loop signature from pickup truck (left) and passenger car (right):
Source [7]

TABLE 1 Classification using magnetic sensor

Total	PV	SUV	Van	Bus	MT	Van, MT
PV 15	11	4				
SUV 7	3	4				
Van 5	1		1			3
Bus 3				3		
MT 7	4	1			2	

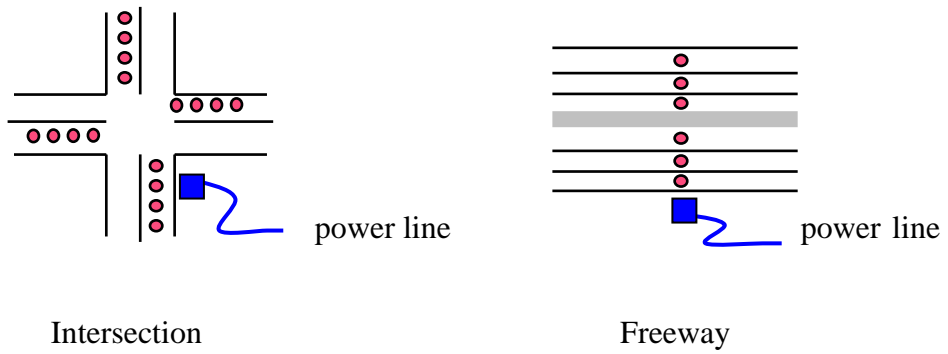


Figure 1 Deploying sensor networks at intersection and freeway

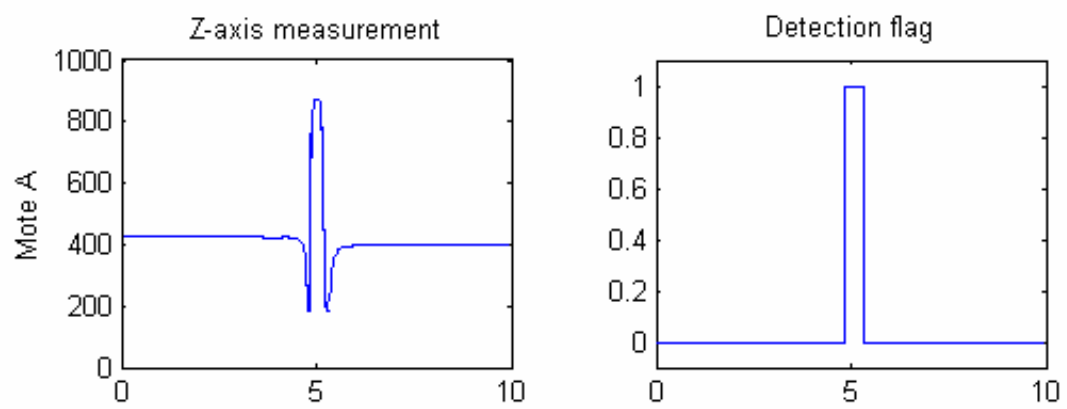


Figure 2 Raw samples and detection flag; time (x-axis) is in seconds

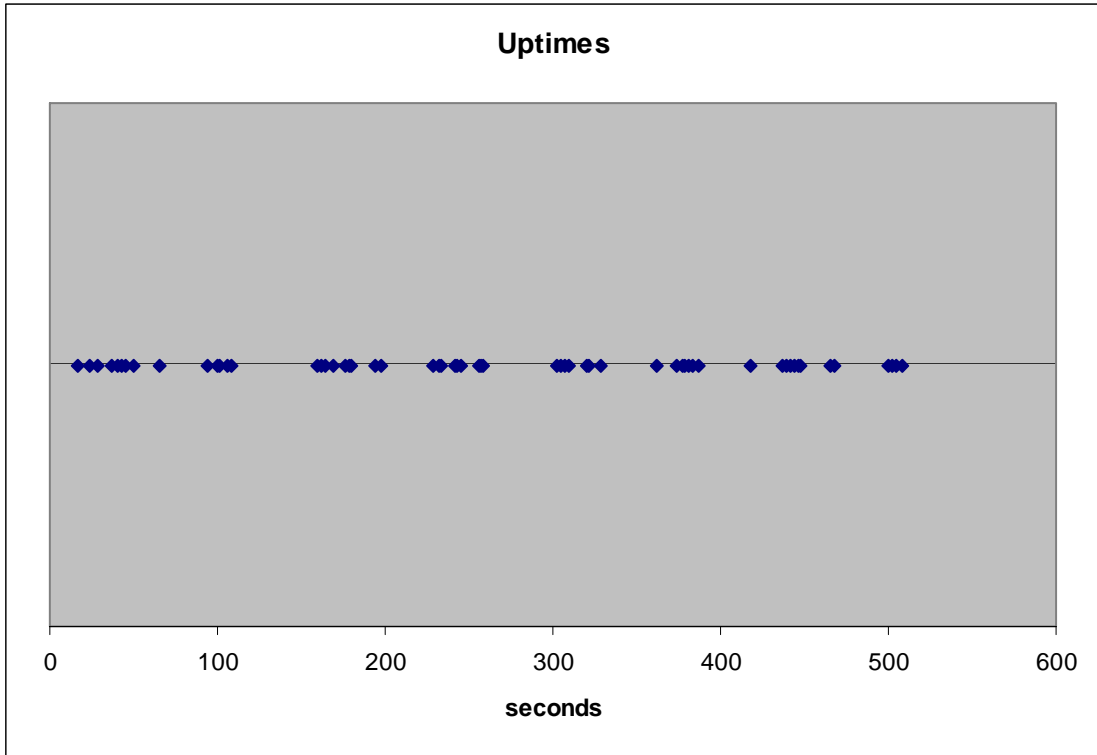


Figure 3 Vehicle arrivals during the first 10 minutes

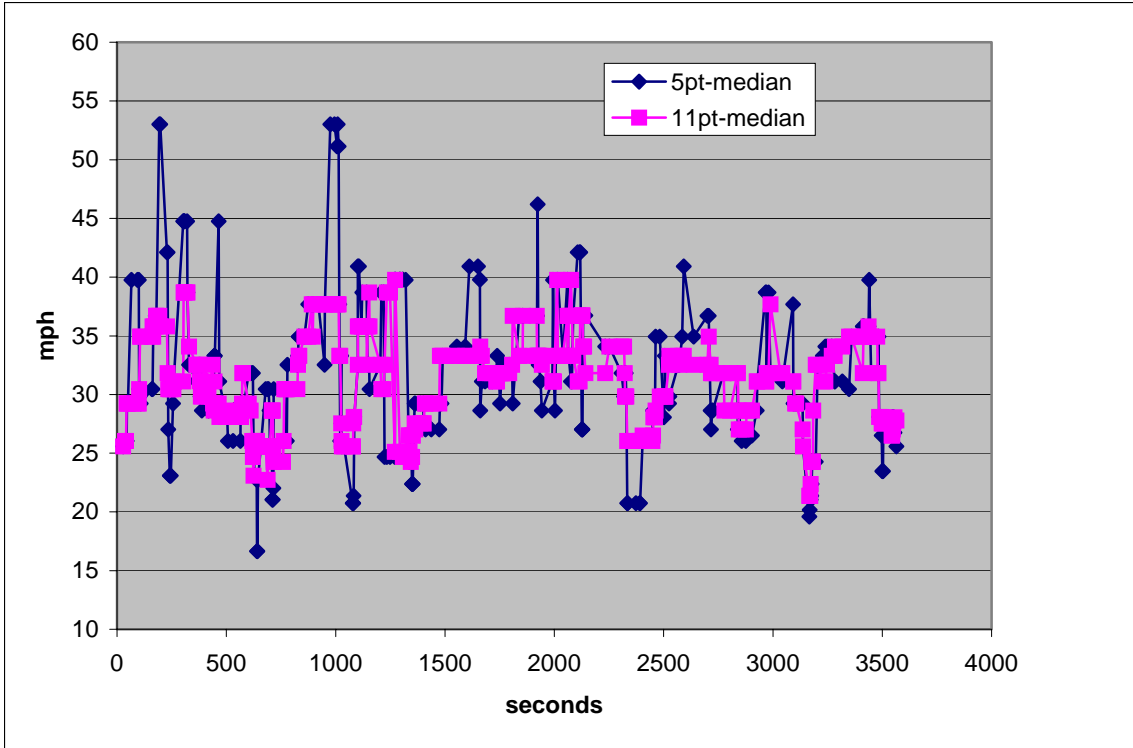


Figure 4 Vehicle speed using 5-point and 11-point median

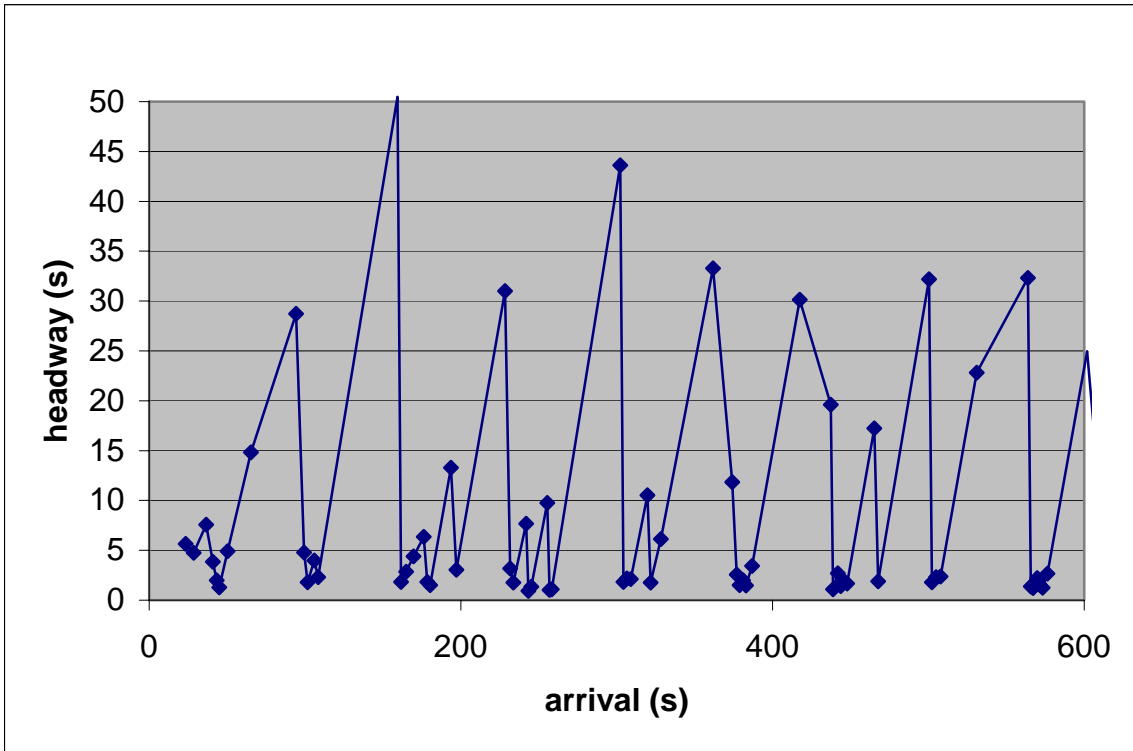


Figure 5 Headway vs. arrival time

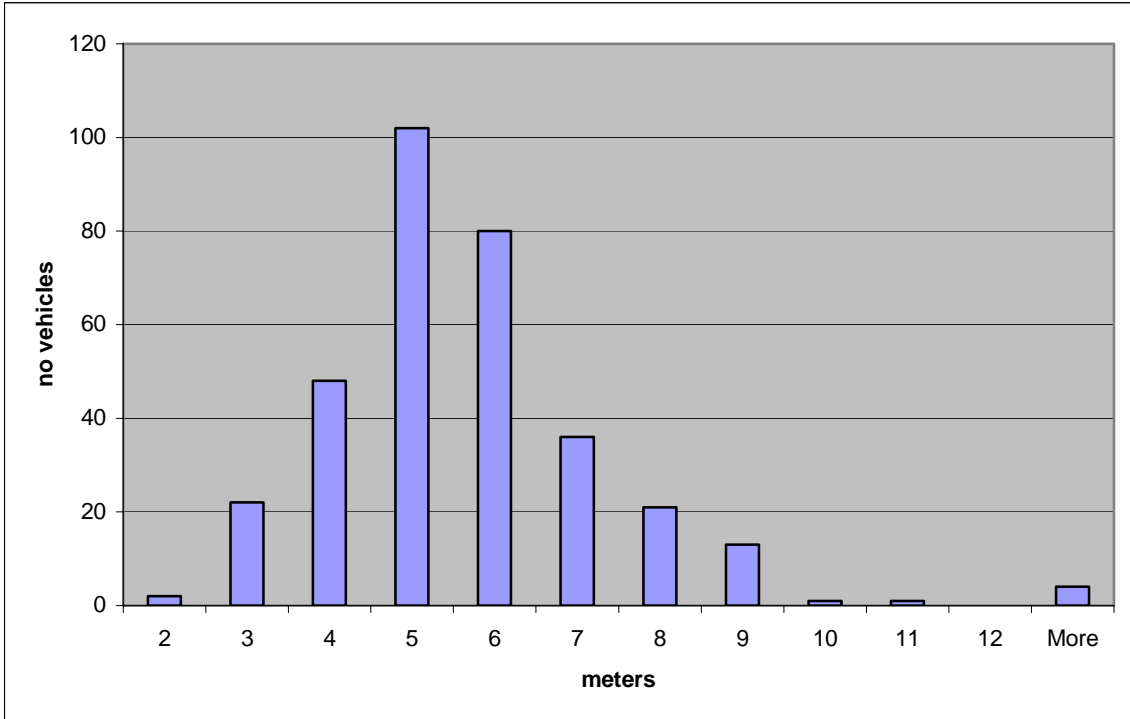


Figure 6 Frequency distribution of vehicle length (m)

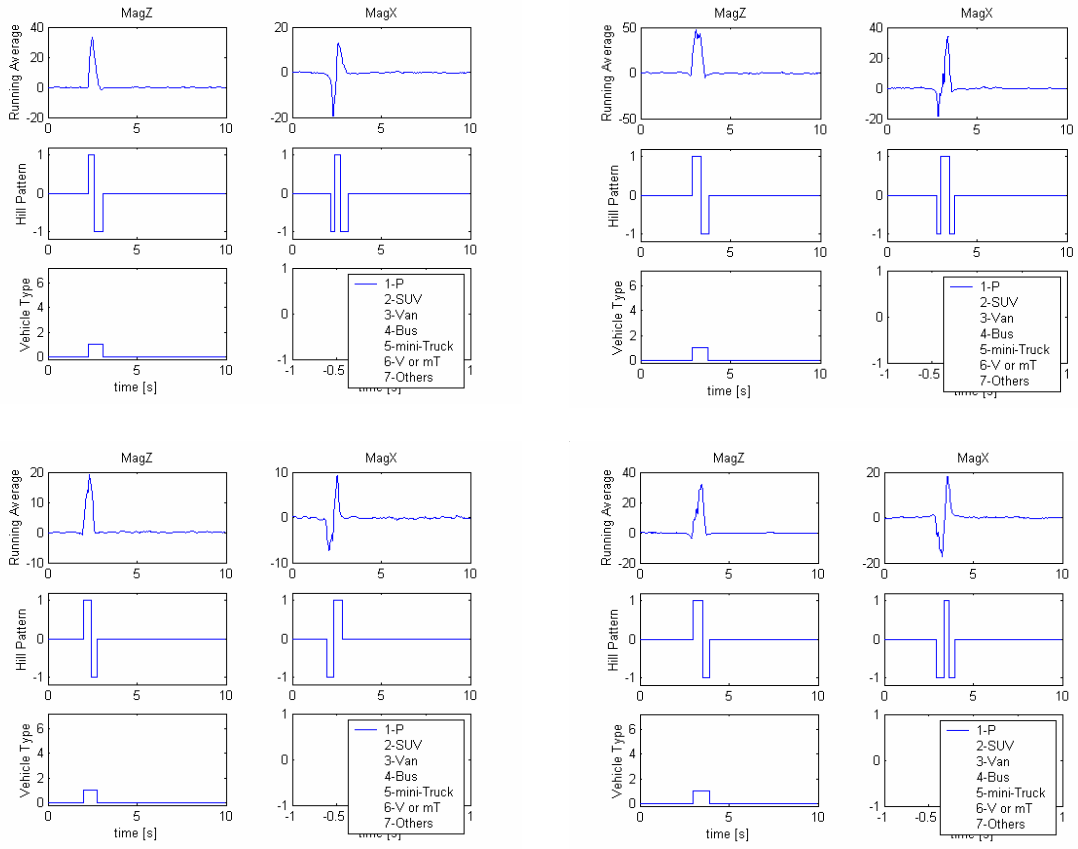


Figure 7 Raw samples and hill pattern from four passenger vehicles

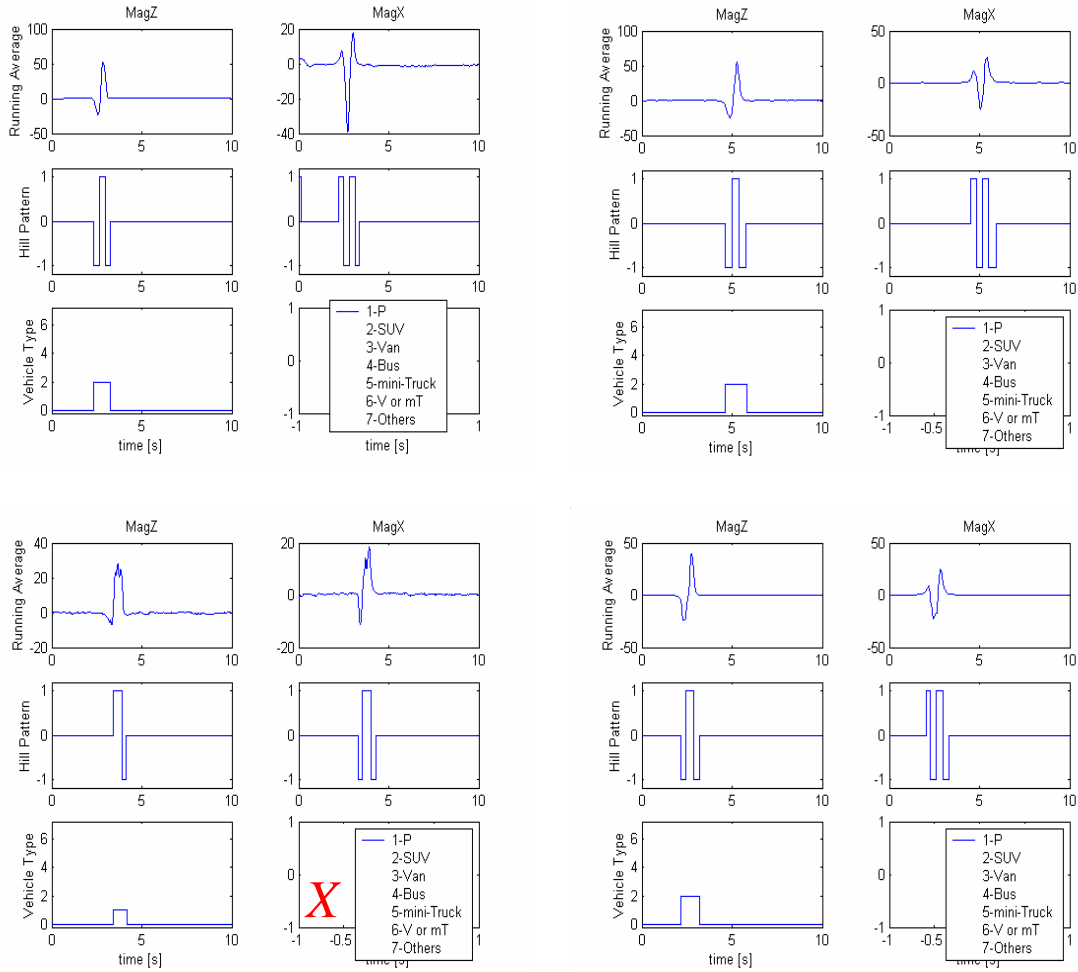


Figure 8 Raw samples and hill pattern from four SUVs

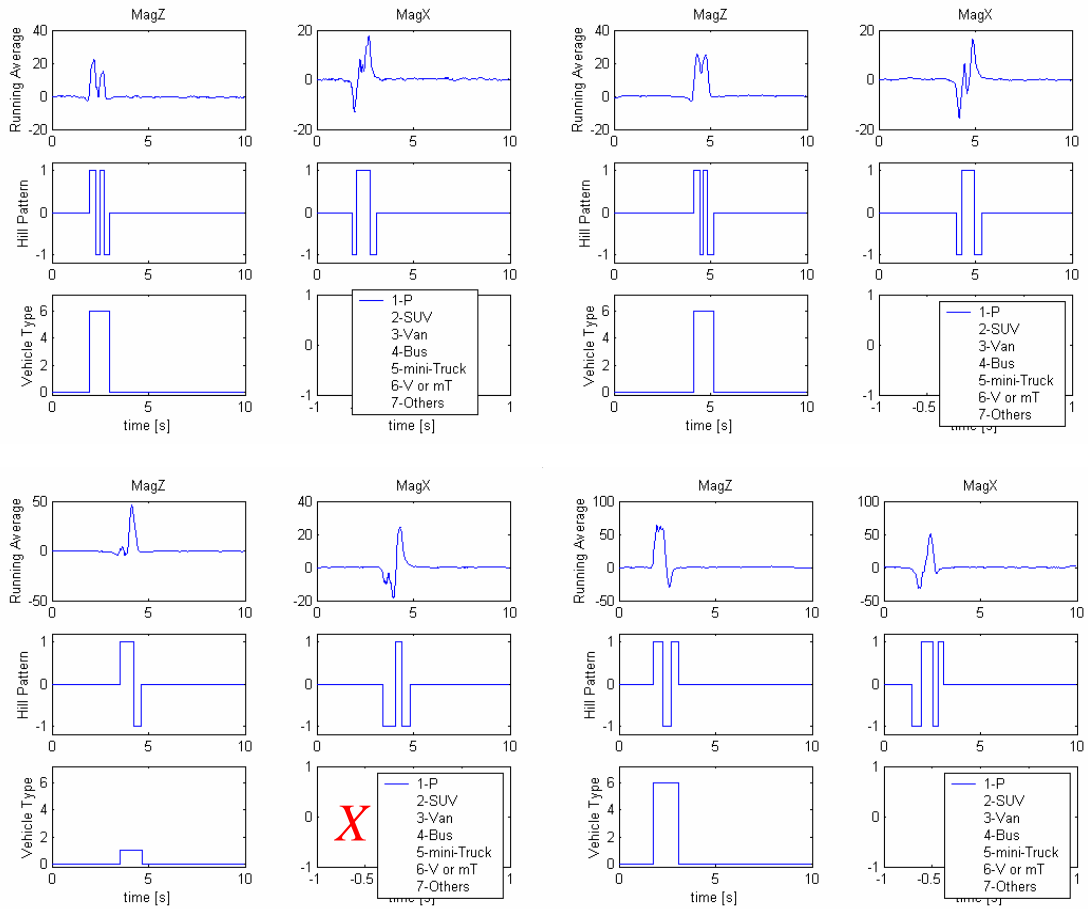


Figure 9 Raw samples and hill pattern from four vans

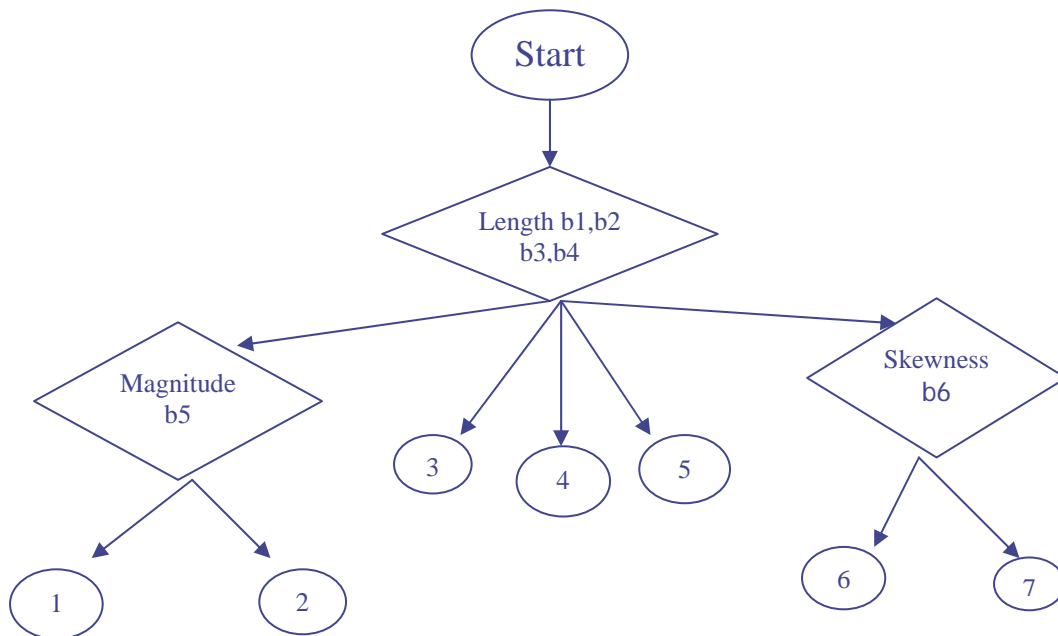


Figure 10 Decision tree for classification into 7 types of vehicles: Source [2]

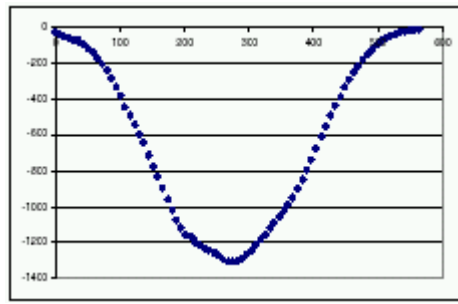
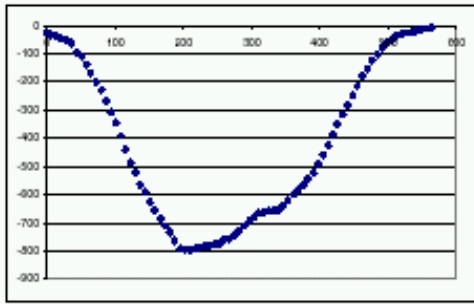


Figure 11 Inductive loop signature from pickup truck (left) and passenger car (right): Source [7]